

Reproducibility Measurements of Three Methods for Calculating In Vivo MR-Based Knee Kinematics

Drew A. Lansdown, MD,¹ Musa Zaid, BS,² Valentina Pedoia, PhD,³
Karupppasamy Subburaj, PhD,⁴ Richard Souza, PT, PhD,³ C. Benjamin, Ma, MD,¹
and Xiaojuan Li, PhD^{1*}

Purpose: To describe three quantification methods for magnetic resonance imaging (MRI)-based knee kinematic evaluation and to report on the reproducibility of these algorithms.

Materials and Methods: T_2 -weighted, fast-spin echo images were obtained of the bilateral knees in six healthy volunteers. Scans were repeated for each knee after repositioning to evaluate protocol reproducibility. Semiautomatic segmentation defined regions of interest for the tibia and femur. The posterior femoral condyles and diaphyseal axes were defined using the previously defined tibia and femur. All segmentation was performed twice to evaluate segmentation reliability. Anterior tibial translation (ATT) and internal tibial rotation (ITR) were calculated using three methods: a tibial-based registration system, a combined tibiofemoral-based registration method with all manual segmentation, and a combined tibiofemoral-based registration method with automatic definition of condyles and axes. Intraclass correlation coefficients and standard deviations across multiple measures were determined.

Results: Reproducibility of segmentation was excellent (ATT = 0.98; ITR = 0.99) for both combined methods. ATT and ITR measurements were also reproducible across multiple scans in the combined registration measurements with manual (ATT = 0.94; ITR = 0.94) or automatic (ATT = 0.95; ITR = 0.94) condyles and axes.

Conclusion: The combined tibiofemoral registration with automatic definition of the posterior femoral condyle and diaphyseal axes allows for improved knee kinematics quantification with excellent in vivo reproducibility.

J. MAGN. RESON. IMAGING 2015;42:533–538.

Understanding knee kinematics is a difficult problem given the complex translational and rotational movements of the knee. The quantification of knee kinematics can provide guidance as to the efficacy of different surgical treatments or rehabilitation programs after injury.¹ Following injury to the anterior cruciate ligament (ACL), altered knee kinematics may be responsible for the observed acceleration of degenerative changes.² In patients with osteoarthritis, alterations in knee kinematics may contribute to disease progression.³

Kinematic magnetic resonance imaging (MRI) has been developed to noninvasively quantify joint kinematics. Previous work has used this tool to describe normal knee kinematics in deep flexion and with axial loading.^{4,5} Reliable

quantification of knee kinematic measurements from MRI requires both reproducible segmentation of bony geometry from MR images as well as an accurate registration method.

We hypothesized that a combined tibiofemoral registration algorithm would offer improved reproducibility over a tibial-based registration system and that an algorithm for automating the definition of necessary regions of interest (ROIs) would allow for similar reproducibility as the combined tibiofemoral registration. Hence, the purpose of this report is to describe and compare three methods for quantification of anterior tibial translation (ATT) and internal tibial rotation (ITR) from kinematic MRI. ATT and ITR were chosen as the primary measurements, as control of these motions are two of the primary functions of the ACL.⁶

View this article online at wileyonlinelibrary.com. DOI: 10.1002/jmri.24790

Received Jul 12, 2014, Accepted for publication Oct 16, 2014.

*Address reprint requests to: X.L., 185 Berry St., San Francisco, CA, 94143. E-mail: xiaojuan.li@ucsf.edu

From the ¹Department of Orthopaedic Surgery, University of California, San Francisco, San Francisco, California, USA; ²School of Medicine, University of California, San Francisco, San Francisco, California, USA; ³Musculoskeletal and Quantitative Imaging Research, Department of Radiology and Biomedical Imaging, University of California, San Francisco, San Francisco, California, USA; and ⁴Singapore University of Technology and Design, Singapore
Contract grant sponsor: NIH/NIAMS; Contract grant number: P50 060752.

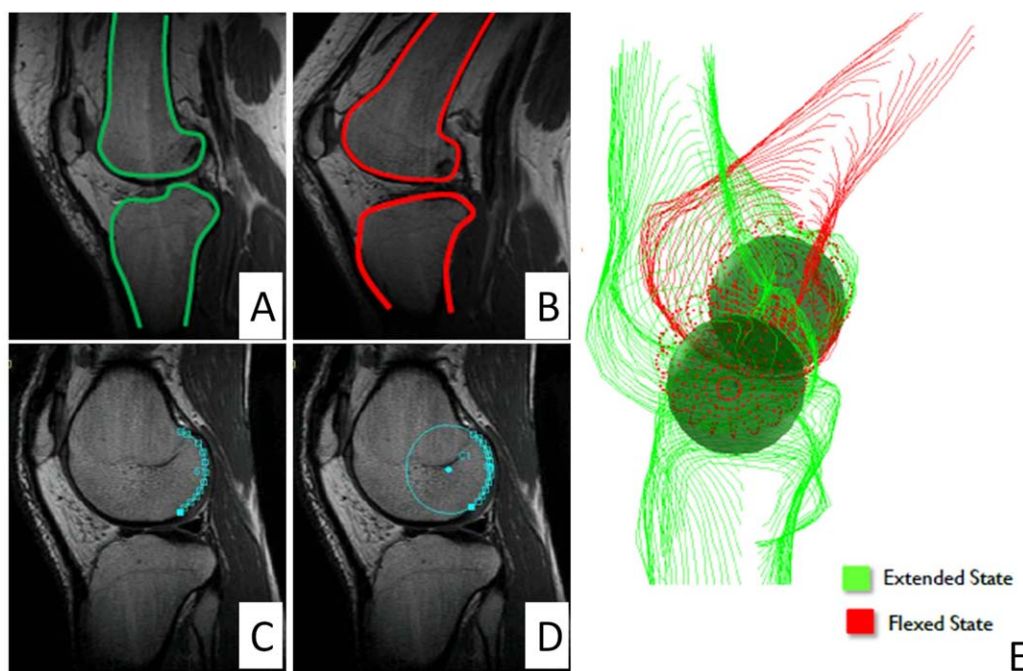


FIGURE 1: Representative segmentations of the tibia and femur in (A) extension and in (B) flexion, and examples of (C) manually defined posterior femoral condyle and (D) automatic segmentation of posterior condyle from previously defined femur segmentation, with (E) 3D reconstruction and modeling of femoral condyles as spheres.

Materials and Methods

Subjects

Six subjects volunteered to participate and provided informed consent prior to image acquisition. Subjects had no history of previous knee surgery, inflammatory arthritis, or degenerative changes. There were three female subjects and three male subjects, with mean ages of 26.7 ± 0.82 years and weight of 75.6 ± 11.2 kg. All procedures were approved by our Institutional Review Board, and all subjects provided written informed consent.

Image Acquisition

Sagittal T_2 fast-spin echo images of the knee were acquired on a wide-bore 3T MR scanner (GE Healthcare; Waukesha, WI) with an 8-channel knee coil (Invivo, Orlando, FL) as previously described.^{7,8} Imaging parameters included: repetition time = 4000 msec; echo time = 48.16 msec; number of averages = 2; field of view = 20 cm; slice thickness = 1.5 cm; matrix size = 512×512 ; pixel size = 0.39×0.39 mm; acquisition time = 2 minutes, 24 seconds. The knee was scanned first in extension, followed by scanning at $\sim 40^\circ$ of flexion. In both positions, the lower extremity was axially loaded with 25% of body weight using a low-friction pulley system.^{1,9} Next, the patient exited the scanner, was then repositioned in a similar fashion, and rescanned in the extended and flexed positions.

Image Processing/Segmentation

Images were segmented semiautomatically (Fig. 1) using in-house MatLab-based software (MathWorks, Natick, MA) by two individuals (D.A.L., M.Z.), each with an experience with the described protocols of more than 30 knees segmented. The cortical margin of the tibia and femur were defined for images extension and flexion. An arc was segmented along the posterior aspect of each femo-

ral condyle in both flexion and extension. The cloud points for the tibial, femoral, and condylar segmentations were interpolated as Bezier splines. The longitudinal axes of the femur and tibia were defined manually by a single line for each bone, drawn near the mid-sagittal aspect of each bone. All segmentations were defined for both the first and second scans for each subject and repeated for the first scan, with a minimum of 1 week between repeating image segmentation for the same patient.

Automatic Posterior Condyle Delineation

The posterior aspect of the femoral condyle was defined automatically for the extended femur segmentation by finding an arc of the circle of best fit on each slice. Starting with the most posterior point of the segmented femur, the first derivative of the segmented points was calculated moving both superiorly and inferiorly as the change in vertical displacement divided by the change in horizontal displacement for the points. The stopping point for the segmentation was chosen as the derivative approached zero. In order to preserve only points on the medial and lateral condyles, the anterior–posterior movement of the posteriormost point of the femur segmentation was calculated between each slice. Segmentation was removed from the intercondylar notch when there were differences greater than 1 mm at the posterior point between slices.

Automatic Diaphyseal Axes Definition

The longitudinal axes of the tibia and the femur were defined automatically according to the centroids of two defined points in the diaphysis of each. First, for both the tibia and the femur, the superior–inferior length of the segmentation was used to find only those slices in the mesial aspect of the bone by finding slices with superior–inferior ranges greater than the median of all segmented slices. To eliminate the metaphyseal and epiphyseal portions of

TABLE 1. Regions of Interest Required for Each Quantification Method With Approximate Time Required per Segmentation

	Region of Interest	Time Required (Min)	Tibial-Based	Combined TF with Manual Condyles/Axes	Combined TF With Auto Condyles/Axes
<i>Extension</i>	Tibia	45	X	X	X
	Femur	20		X	X
	Condyles	10	X	X	
	Diaphyseal Axis	2	X	X	
<i>Flexion</i>	Tibia	45	X	X	X
	Femur	20		X	X
	Condyles	10	X		
	Diaphyseal Axes	2	X	X	
Total segmentation time (min)			114	144	130
Registration performed	Tibia in flexion to tibia in extension		X	X	X
	Femur in flexion to femur in extension			X	X

TF, tibiofemoral.

each, the distal one-third of the femoral segmentation and proximal one-half of the tibial segmentation were excluded. The centroids of the each half of the remaining femur segmentation and the superior and inferior third of the remaining tibial segmentation were calculated. The longitudinal, diaphyseal axes were defined as the lines connecting these points. All automatic condylar segmentations and diaphyseal axes were inspected visually. No points were adjusted, removed, or added prior to kinematic calculations.

Tibial-Based Registration Calculation^{7,8}

The tibia in flexion was registered to the tibia in extension using an iterative closest point algorithm (ICP), and the transformation matrix was applied to the segmentation of the femoral condyles in flexion. Next, the medial–lateral axis of a tibial-based coordinate system was established as the line connecting the posteriormost points of the medial and lateral tibial plateaus, with the tibial origin set as the mid-point of this line. The superior–inferior axis was obtained from the user-defined long axis of the tibia, and the anterior–posterior axis was calculated as the cross product of these axes. This process was performed for the extended and flexed tibial segmentations.

The manual segmentations of the posterior aspect of the medial and lateral femoral condyles were then used to model the condyles as spheres. The center of each sphere represented the center of rotation for the femoral condyles, and the line connecting these points defined the medial–lateral axis of the femoral coordinate system with the femoral origin set as the mid-point between the centers of the medial and lateral femoral condylar spheres. The user-defined long axis of the femur was the superior–inferior axis of the femoral coordinate system, and the anterior–posterior axis was defined as the cross product of these two lines. This process was performed for the femur in both the extended and flexed positions.

The tibial position relative to the epicondylar axis of the femur was calculated as the anterior–posterior difference in the origins of the tibial axis and femoral axis in both the extended ($\text{Position}_{\text{Ext}}$) and flexed ($\text{Position}_{\text{Flex}}$) positions. The rotational alignment of the tibia was calculated as the angle between the medial–lateral axis of the tibia and the medial–lateral axis of the femur in the extended ($\text{Rotation}_{\text{Ext}}$) and flexed ($\text{Rotation}_{\text{Flex}}$) positions. ATT was determined as the difference in the tibial position between flexion and extension ($\text{ATT} = \text{Position}_{\text{Flex}} - \text{Position}_{\text{Ext}}$), and ITR was calculated as the difference in tibial rotation between flexion and extension ($\text{ITR} = \text{Rotation}_{\text{Flex}} - \text{Rotation}_{\text{Ext}}$).

Combined Tibiofemoral Registration

The tibial axis was defined as outlined above.

The femoral condyles were modeled as spheres in only the extended position using the femoral condyle segmentation as described above. Next, the ICP was used to register the flexed femur segmentation to the extended femur. The transformation matrix was then applied to the spheres representing the femoral condyles. Similar calculations as above were then used to determine the ATT and ITR.

Kinematic Calculations and Statistics

Quantification of ATT and ITR was performed for each scan using all three methods outlined in Table 1. The reproducibility was assessed for multiple segmentations (two attempts by each segmenter) and scan/rescan by using an average measures intraclass correlation coefficient (ICC). Mean values and standard deviations for segment, resegment, and rescan were calculated for each method, with comparisons of each attempt by method made using an analysis of variance (ANOVA) test. The differences in ATT and ITR between left and right knees were calculated. The standard error of the measurement (SEM) was calculated for ATT and ITR.

TABLE 2. Intraclass Correlation Coefficient and Standard Errors of the Mean for Three Algorithms for Determination of Knee Kinematics

	Tibial		Combined TF With Manual Condyles/Axes		Combined TF With Automatic Condyles/Axes	
	ATT	ITR	ATT	ITR	ATT	ITR
Intraclass Correlation Coefficients						
Segment-resegment	0.95	0.97	0.98	0.99	0.98	0.99
Scan-rescan	0.89	0.86	0.94	0.94	0.95	0.94
Standard Errors of the Measurement						
Segment-resegment	0.31 mm	0.67°	0.19 mm	0.42°	0.19 mm	0.4°
Scan-rescan	0.48 mm	1.51°	0.34 mm	0.96°	0.31 mm	0.94°

ATT, anterior tibial translation; ITR, internal tibial rotation; TF, tibiofemoral.

The root mean square (RMS) was used to summarize standard deviations by method and the left–right differences in ATT and ITR. Statistical analyses were performed with Stata (StataCorp, College Station, TX).

Results

The ICC for all three quantification methods for ATT and ITR ranged from 0.86 to 0.99, with the highest values observed with the combined tibiofemoral (TF) registration using either manual or automatic condylar/axis segmentation (Table 2). The highest ICCs were obtained with the combined TF registration. The ICCs for resegmenting the same dataset were higher than those for quantifying ATT and ITR for repeat scans of the same patient.

ATT values for each knee by quantification method are displayed in Fig. 2, and ITR values for each knee are displayed in Fig. 3. There were no statistically significant differences between mean values for ATT across segment/resegment or rescan for the tibial-based (segment: 0.89 ± 1.44 mm, resegment: 0.38 ± 1.58 mm, rescan: 0.78 ± 1.51 ; $P = 0.47$), TF with manual condyles/axes (segment: 0.72 ± 1.27 mm, resegment: 0.58 ± 1.45 mm, rescan: 0.65 ± 1.5 mm; $P = 0.94$), or TF with automatic condyles/axes (segment: 0.48 ± 1.28 mm, resegment: 0.55 ± 1.36 mm; rescan: 0.66 ± 1.50 mm; $P = 0.90$). There were also no statistically significant differences between mean values for ITR across segment/resegment or rescan for tibial-based (segment: $10.85 \pm 4.48^\circ$, resegment: $11.08 \pm 4.07^\circ$, rescan: $9.79 \pm 3.57^\circ$; $P = 0.51$), TF with manual condyles/axes (segment: $10.48 \pm 4.22^\circ$, resegment: $10.40 \pm 4.22^\circ$, rescan: $9.51 \pm 3.59^\circ$; $P = 0.65$), or TF with automatic condyles/axes (segment: $10.63 \pm 4.14^\circ$, resegment: $10.46 \pm 4.13^\circ$, rescan: $9.74 \pm 3.55^\circ$; $P = 0.71$).

The SEMs were lower for combined tibiofemoral registration compared to tibial-based registration (Table 2). The RMS for standard deviations were lowest for combined

TF quantification using automatic condyles/axes (0.31 for ATT and 0.74 for ITR) as compared with combined TF with manual segmentation (0.33 for ATT and 0.84 for ITR) and tibial-based quantifications (0.71 for ATT and 1.58 for ITR). The RMS for mean differences in the left and right knees for the same subject were 1.02 mm for ATT and 3.94° for ITR using tibial-based quantification; 0.83 mm for ATT and 4.13° for ITR using combined TF quantification with manual condyles/axes; and 0.98 mm for ATT and 4.16° for ITR using combined TF quantification with automatic condyles/axes.

Discussion

This study aimed to describe the quantification algorithms and their reproducibility for determining MR-based tibiofemoral kinematics. All three methods described here offer high levels of reproducibility for multiple scans and repeated segmentations. The clinical interpretation of the SEM

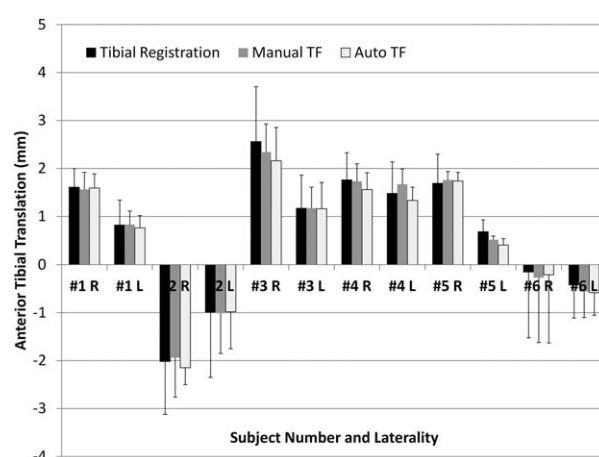


FIGURE 2: Anterior tibial translation values for each subject according to the processing algorithm. L = left knee; R = right knee.

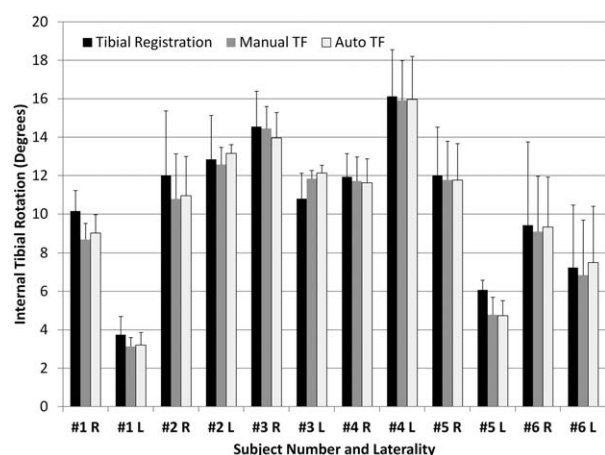


FIGURE 3: Anterior tibial translation values for each subject according to the processing algorithm. L = left knee; R = right knee.

indicates that one can be 95% confident that the outcomes measured on one day are within 0.62 mm for ATT and 1.9° for ITR (2*SEM) of the measurements from another day when using the combined TF quantification with automatic condyles/axes definition. This offers an improvement over our previous tibial-based quantification method with 95% confidence intervals of 0.96 mm for ATT and 3.02° for ITR.

The combined TF algorithms outperformed the tibial-based quantification method, due to increased points for registration from the femur segmentation and that the posterior condyles are only segmented in the extended position. The addition of an automated method to determine the posterior condylar segmentation and diaphyseal axes performs at least as well as the quantification with manually defined ROIs. The elimination of the need for posterior condylar segmentation saves segmentation time without compromising the reproducibility.

Establishing reference values for expected intrasubject differences between left and right knees will aid in comparisons of MR-based kinematics between injured and contralateral knees. Given the current methods and configuration, the ATT falls within ~1 mm and ITR within ~4°. This variation incorporates both the differences introduced from repositioning the subject, from segmentation, and from side-to-side differences within a subject.

The reproducibility of these current methods compares favorably with prior reports. Open dynamic MRI of the knee allows for accuracy within 1.5 mm for translational measurements, although allowed for bending up to 90°. ¹⁰ MRI combined with dual-planar fluoroscopy can produce a 3D model that is matched to fluoroscopic views during motion with standard deviations in positional measurements of less than 0.1 mm. ^{11,12} This fluoroscopic technique does require minimal exposure to ionizing radiation and the availability of two fluoroscopy machines. Also, the 4 hours

of acquisition time and 8 hours of processing time per knee are much longer than the process presented here. Motion analysis has been used in multiple other studies with excellent reproducibility with precision up to 0.1 mm and 0.3°, but this process requires specialized equipment and does not allow for a combined assessment of articular cartilage and whole-joint health. ¹³ MRI, fluoroscopy, and motion analysis can also all be combined for a multimodal evaluation of knee kinematics. ¹⁴

This report should be interpreted with an understanding of our limitations. First, there is a reference standard to provide a reference value for ATT and ITR. Only patients with normal knees were included in this current study to understand the expected variability in a normal knee, but the absence of reproducibility measurements for injured knees is also a limitation of this study. A ligamentous injury, such as an ACL tear, however, should not affect the bony segmentation or the automatic definition of the condyles or axes. Also, while the purpose of the kinematic imaging is to evaluate knee motion, the protocol consists of obtaining two static images. Unlike other kinematic methods, this protocol does not allow for deep bending to 90° or beyond. We did not evaluate a dynamic process, but rather obtained measurements at two set positions.

In conclusion, the current study offers three quantification methods for determining tibiofemoral kinematics. The results demonstrate high reproducibility across both multiple segmentations and repeat scans, especially the method with combined tibia-femur registration and with automatic determination of the posterior condyles and diaphyseal axes.

References

1. Schairer WW, Haugom BD, Morse LJ, Li X, Ma CB. Magnetic resonance imaging evaluation of knee kinematics after anterior cruciate ligament reconstruction with anteromedial and transtibial femoral drilling techniques. *Arthroscopy* 2011;27:1663–1670.
2. Andriacchi TP, Mundermann A, Smith RL, Alexander EJ, Dyrby CO, Koo S. A framework for the in vivo pathomechanics of osteoarthritis at the knee. *Ann Biomed Eng* 2004;32:447–457.
3. Farrokhi S, Voycheck CA, Klatt BA, Gustafson JA, Tashman S, Fitzgerald GK. Altered tibiofemoral joint contact mechanics and kinematics in patients with knee osteoarthritis and episodic complaints of joint instability. *Clin Biomech* 2014;29:629–635.
4. Patel VV, Hall K, Ries M, et al. A three-dimensional MRI analysis of knee kinematics. *J Orthop Res* 2004;22:283–292.
5. Johal P, Williams A, Wragg P, Hunt D, Gedroyc W. Tibio-femoral movement in the living knee. A study of weight bearing and non-weight bearing knee kinematics using 'interventional' MRI. *J Biomech* 2005;38:269–276.
6. Beynon BD, Johnson RJ, Abate JA, Felming BC, Nichols CE. Treatment of anterior cruciate ligament injuries, Part 1. *Am J Sports Med* 2005;33:1579–1602.
7. Shefelbine SJ, Ma CB, Lee KY, et al. MRI analysis of in vivo meniscal and tibiofemoral kinematics in ACL-deficient and normal knees. *J Orthop Res* 2006;24:1208–1217.

8. Carpenter RD, Majumdar S, Ma CB. Magnetic resonance imaging of 3-dimensional in vivo tibiofemoral kinematics in anterior cruciate ligament-reconstructed knees. *Arthrosc J Arthrosc Relat Surg* 2009;25: 760–766.
9. Haugom B, Schairer W, Souza RB, Carpenter D, Ma CB, Li X. Abnormal tibiofemoral kinematics following ACL reconstruction are associated with early cartilage matrix degeneration measured by MRI T1rho. *Knee* 2012;19:482–487.
10. Logan MC, Williams A, Lavelle J, Gedroyc W, Freeman M. Tibiofemoral kinematics following successful anterior cruciate ligament reconstruction using dynamic multiple resonance imaging. *Am J Sports Med* 2004;32:984–992.
11. Kozanek M, Hosseini A, Liu F, et al. Tibiofemoral kinematics and condylar motion during the stance phase of gait. *J Biomech* 2009;42: 1877–1884.
12. Li G, Van de Velde SK, Bingham JT. Validation of a non-invasive fluoroscopic imaging technique for the measurement of dynamic knee joint motion. *J Biomech* 2008;41:1616–1622.
13. Dyrby CO, Andriacchi TP. Secondary motions of the knee during weight bearing and non-weight bearing activities. *J Orthop Res* 2004; 22:794–800.
14. Taylor KA, Terry ME, Utturkar GM, et al. Measurement of in vivo anterior cruciate ligament strain during dynamic jump landing. *J Biomech* 2011;44:365–371.